First publ. in: Chemical Physics Letters 217 (1994), 5-6, pp. 600-604

Shell structure and s–p hybridization in small aluminum clusters

G. Ganteför and W. Eberhardt
Institut für Festkörperforschung, Forschungszentrum Jülich, 5170 Jülich, Germany

Photoelectron spectra of Al_n^- (n=2–20) clusters are presented. Due to the improved energy resolution and the relatively high photon energy ($h\nu$=6.424 eV, ArF laser radiation) available in our experiment the spectra reveal the mechanism of the onset of the s–p hybridization occuring in these particles. Between Al_6^-–Al_{12}^- a mixing of the uppermost antibonding 3s derived orbital with the 3p band takes place which is observed simultaneously with the 2D→3D structural transition predicted for Al clusters in this size range. Starting from Al_{13}^- a pattern resembling an electronic shell structure is identified.

1. Introduction

The properties of small metal particles are a matter of increasing interest both in basic research of physics and chemistry and in various applications like microelectronics and catalysis. The electronic and geometric structure (see e.g. ref. [1]) does not change gradually from atomic and molecular behaviour to the bulk properties but abrupt changes are observed in the properties depending on the size range.

One important observation in cluster science are shell effects. These can include shells of atoms, such as the icosahedral shell in rare gas clusters [2], and shells of electrons observed in e.g. monovalent metal clusters [3]. The electronic shell model [3] (jellium model) can describe various properties of monovalent metal clusters such as the alkali and coinage (Cu, Ag, Au) metal clusters. However, metal clusters with a higher number of valence electrons per atom, like aluminum [4,5], exhibit properties which cannot be explained in terms of the jellium model (JM). A possible reason for this discrepancy is the lack of overlap between the 3s and 3p derived electronic states in the valence band of small Al clusters [6].

The electronic configuration of the Al atom is (Ne) $3s^2 3p$. The binding energy (BE) of the 3s orbital is about 6.4 eV higher than the BE of the outermost 3p orbital [4,7]. For bulk Al, 3s and 3p derived states are completely merged into the s–p hybridized valence band with nearly perfect free electron properties (see e.g. ref. [8]). In the clusters the two bands are expected to broaden starting from the atomic orbitals into bonding and antibonding orbitals. This behaviour is schematically displayed in fig. 1.

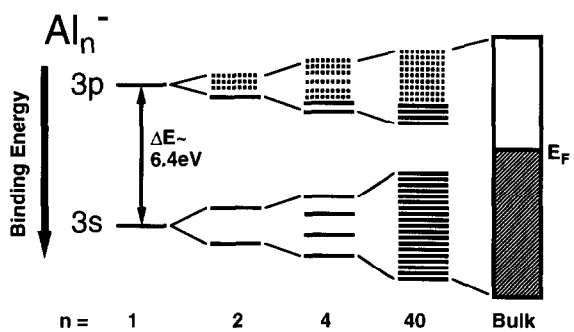

Fig. 1. Schematic display of the electronic level structure of the valence band of the Al atom, clusters and Al bulk metal in the neutral electronic ground state. The binding energy refers to the vacuum level. Occupied single particle orbitals (n=1, 2, 4) are displayed by bars, unoccupied ones by dashed bars. The two 3s electrons are at about 6.4 eV higher BE than the uppermost single electron occupying the 3p orbital. With increasing number of atoms n the number of 3s and 3p derived molecular orbitals increases and the two bands broaden. For n=40 and bulk Al the occupied and unoccupied density of states is displayed by hatched and open rectangles, respectively. The gap between the two manifolds of states decreases and in the valence band of bulk Al the 3s and 3p density of states in completely hybridized. The BE of the highest occupied molecular orbital (HOMO) corresponds to the Fermi energy E_F in bulk metal.

The 3s–3p gap is expected to decrease and at a certain cluster size the two bands merge. The cluster size when this occurs is still a matter of discussion and is estimated to be around 40 atoms [9,10].

In a recent high-resolution photoelectron experiment [4] on Al_n^- ($n=2$–15) we identified three size ranges with different patterns in the spectra. These patterns can be understood using the following assumptions: The smallest particles up to $n=5$ are planar and the electronic structure is governed by σ and π orbitals. Beyond $n=5$ up to $n=11$ a transition from two-dimensional to three-dimensional structures takes place. Starting from Al_{12}^- the particles are compact and approaching a spherical shape.

In the present Letter we try to address two issues: (1) the onset of s–p hybridization and (2) the question whether any indication of a shell structure can be found in the photoelectron spectra of the larger clusters. To obtain information about the hybridization we recorded spectra using a higher photon energy ($h\nu=6.424$ eV, ArF excimer laser) than in previous work [4]. The study is extended to somewhat larger clusters (up to $n=20$) and the spectra with $n>13$ are analyzed to identify any electronic shell structure.

2. Experimental

The experimental apparatus is described in detail elsewhere [11]. The Al_n^- clusters are generated using a PACIS (Pulsed Arc Cluster Ion Source). The anions are accelerated after passing the skimmer using a pulsed electric field. The anion beam is directed into a time of flight electron spectrometer. A selected bunch of anions is hit by a UV-laser pulse resulting in the detachment of electrons. The kinetic energy of these electrons is measured using a "magnet bottle" type [12] time-of-flight spectrometer.

The energy resolution depends on the kinetic energy of the electrons and the velocity of the anions (Doppler broadening) and varies between 20–300 meV. At the high photon energy used in the experiment ($h\nu=6.424$ eV) scattered light creates a background electron signal resulting in a rather poor signal-to-noise ratio. The anion intensity is increased by choosing a higher anion beam energy which is accompanied by a loss of resolution (100–300 meV).

The intensity of the emitted electrons is recorded as a function of the binding energy (BE), which is calculated as the difference between the photon energy and the kinetic energy of the electrons. The maximum BE is the difference between the photon energy ($h\nu\approx6.4$ eV) and the low-energy transmission limit of the electron spectrometer (0.4 eV).

3. Results and discussion

Fig. 2 displays the electron emission spectra of Al_n^- clusters with $n=2$–20. The spectra agree well with earlier data [4,9,13] except for the differences

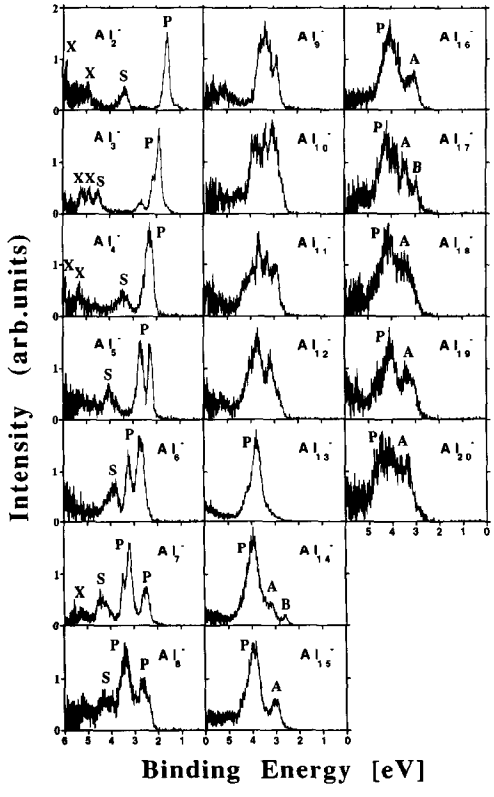

Fig. 2. Photoelectron spectra of Al_n^- ($n=2$–20) taken with $h\nu=6.242$ eV (ArF excimer laser radiation). The energy resolution varies between 0.1–0.3 eV. Features assigned to photoemission from 3s and 3p derived orbitals are marked s and p, respectively. Features assigned to the electronic shell above the closed shell corresponding to peak P of Al_{13}^- are marked A and B.

due to the higher photon energy ($h\nu = 6.424$ eV), energy resolution and signal-to-noise ratio. Thus the gap between the 3p and 3s derived orbitals corresponding to a low photoemission signal at high BE (5–6 eV) can be studied. The signal-to-noise ratio and the energy resolution are not quite as good as in our spectra taken at lower photon energy ($h\nu = 5$ eV, ref. [4]). However, the spectra shown here extend over a broader range and reveal many more details than the earlier data [9] taken at high photon energy.

For the discussion of the s–p hybridization the features displayed in fig. 2 have to be assigned to photoemission from 3s and 3p derived orbitals. As discussed in detail in our previous publication [4] features up to 4.5 eV BE have been assigned. For the small clusters ($Al_2^- - Al_5^-$) the assignments result from the comparison [4,14] with calculations. In general, 3s and 3p derived orbitals can be distinguished by a comparison [4] with similar data on Ga_n^- clusters. For Ga, the 4s derived orbitals exhibit a higher BE (by ≈ 1 eV) due to the higher BE of the 4s orbital in the Ga atom with respect to Al. These assignments are included in fig. 2 (marked s,p). Features beyond 4.5 eV BE cannot be unambiguously assigned (marked X). Presumably these are of 3s character, however multielectron excitations (shake-up) might also contribute to the spectral density in this region.

The range of BEs of the 3p derived features ("3p band") and the BE of the single 3s derived peak (fig. 2) are visualized in fig. 3. For each cluster the BE of the upper and lower BE edge of the 3p band is plotted. If the 3p band is resolved into single transitions the positions of the peaks located at the lowest and the highest BE within the band are taken as the edges. For the Al atom there is only one 3p orbital and therefore the bandwidth is zero as displayed in fig. 3. The BE of the two electrons occupying the 3p orbital in the anion is equal to the electron affinity of the atom (≈ 0.45 eV [15]). For the dimer the occupied 3p derived σ and π orbitals are nearly degenerate resulting again in a zero bandwidth.

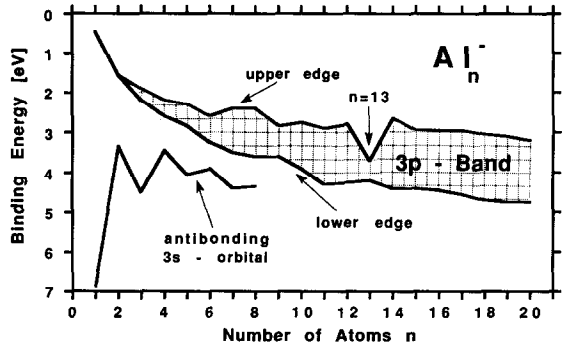

Fig. 3. The bandwidth of the 3p band in Al_n^- with $n = 2$–20 extracted from the photoelectron data displayed in fig. 2. The position of a single peak assigned to the uppermost antibonding orbital of the 3s band is included in the figure for $Al_2^- - Al_8^-$. The binding energies of the 2s and 3p orbitals of Al_1^- are taken from the literature [7,15].

Beyond $n = 11$ the 3p band consists of a single broad feature (fig. 2, marked P) accompanied in some cases by smaller peaks at the low BE side (fig. 2, marked A, B). For these clusters the position of the feature at the lowest BE is taken as the value of the upper 3p band edge. This value is also equal to the vertical electron detachment energy [4] (VDE). At the high BE edge we take the intersection of the corresponding slope of the main broad peak with the background and subtract 0.25 eV from this value in order to account for the limited experimental resolution.

The BE of the whole band increases with cluster size. This increase can be described by simple electrostatic models [3]. The broadening of the band is monotonous. Only for Al_{13}^- is a pronounced minimum of the bandwidth observed, which is related to the high geometric symmetry [4,5] of this cluster. At this point we want to remind the reader that our data can only reflect the occupied part of the 3p band. The bandwidth including the unoccupied antibonding orbitals is much larger.

Because of the limited photon energy the 3s band cannot be observed in our experiment. The spectra displayed in fig. 2 exhibit a low photoemission signal beyond 5 eV BE, which we assign to the gap between the 3s and 3p derived states. Due to this observation, and in agreement with earlier studies, we conclude that the main parts of the two bands are well separated at least up to Al_{20}^- as schematically illustrated in fig. 1. However, a single 3s derived orbital seems to have an extraordinarily low BE compared to the main part of the 3s band. The BE of this orbital is also included in fig. 3 for $n = 1$–8. For the atom the value of the BE of the 3s level (fig. 3) is taken from the literature [7,15]. With increasing cluster size the

BE of the antibonding 3s orbital approaches the BE of the lower edge of the 3p band, and beyond $n=8$ they merge and are no longer separated.

From fig. 3 the following picture of the onset of s–p hybridization in small Al clusters emerges: For Al_n^- clusters with $n=2$–20 the manifolds of the 3s and 3p derived orbitals are well separated by a gap of more than 1 eV. However, one single particle orbital with predominantly 3s character shifts towards the 3p band with increasing BE and merges with the 3p band beyond $n=9$. Therefore, the onset of the mixing of 3s and 3p derived orbitals in small Al clusters depends on the symmetry of the involved single particle orbitals and starts for a certain 3s orbital at a much smaller cluster size than suggested in earlier contributions [9,10].

The spectra of the larger clusters Al_{13}^-–Al_{20}^- exhibit a simple structure and are similar to each other. One prominent feature (fig. 2, marked P) is observed at 40–4.5 eV BE. This feature is accompanied by one or two smaller peaks (marked A, B) located at the low BE side of the main peak. Only in the spectrum of Al_{13}^- no such smaller peak is observed. The relative intensity of the smaller peaks with respect to the main feature seems to increase with increasing cluster size.

This behaviour resembles an electronic shell structure observed for monovalent metal clusters [3,16]. If we assume Al_{13}^- to be a magic number cluster, feature P observed in the photoelectron spectrum corresponds to a closed electronic shell. In terms of an electronic shell model additional electrons occupy the next shell located at lower BE. This gives rise to features at lower BE with respect to the closed shell peak. With further increasing cluster size the new shell is filled with more and more electrons corresponding to an increasing intensity in the photoelectron spectra.

We can try to measure the occupation of the new shells by comparing the emission intensity at the low BE side to the intensity of the main peak. With each additional atom three valence electrons are added to the cluster valence band. As long as the bands are separated into a 3s and a 3p band, two electrons are filled into the 3s bands and only one is added to the outermost 3p band. On the other hand, if the two bands are completely merged all three electrons would be added to the outermost shell.

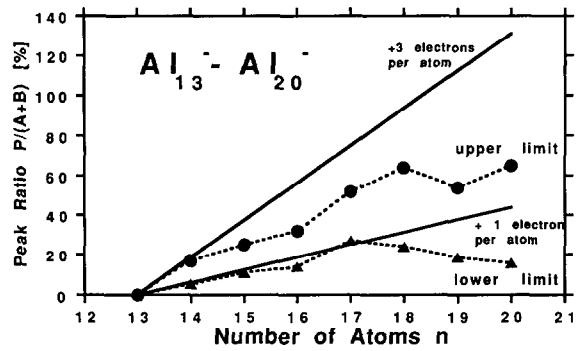

Fig. 4. Upper and lower limit of the intensity ratio ((A+B)/P)) between feature A, B and feature P in the spectra of Al_n^- (fig. 1) with $n=13$–20. The determination of these values is explained in the text.

Fig. 4 displays the ratio between the area of the smaller peaks at low BE and the area of the main peak at about 4 eV BE for clusters with $n=13$–20. Due to the poor signal-to-noise ratio, especially in the case of the larger clusters, the determination of the areas is difficult. We used two different methods to determine the area which result in a lower and an upper limit of the intensity ratio. The upper limit of the ratio is determined by separating the two features at the position of the minimum and integrating each part of the areas separately. This method only gives the correct ratio if both features exhibit equal intensity and lineshape. If one peak is much larger than the other one a certain part of the area below the smaller peak belongs to the shoulder of the larger peak. Thus, the area of the smaller peak is overestimated.

The lower limit of the ratio is determined by fitting the peaks using Lorentzian functions. The Lorentzians exhibit extended tails and therefore the area of the smaller feature located at the tail of the larger peak coresponds mostly to the tail of the larger peak. We assume that a Lorentzian shape of the features is the worst case which therefore yields the lower limit of the intensity ratio.

The calculated ratios for the two different possibilities (one or three electrons increase per atom) are also displayed in the figure. For the calculated values we assumed equal detachment cross section for both involved electronic shells. Also we assumed the number of electrons in the closed shell of Al_{13}^- to be 16 (=13+1 3p electrons and 2 3s electrons).

According to fig. 4 the intensity increase of the new feature corresponds to one electron per additional Al atom. It seems likely that the 3p orbital of each additional Al atom merges into the shell at lowest BE. Therefore, the two separated peaks observed in the spectrum of e.g. Al_{19}^- (fig. 2) can be assigned to two different electronic shells. Conversely, feature P in the spectra of Al_n^- with $n=13$–20 is assigned to the shell filled with 16 electrons (two 3s and fourteen 3p electrons) observed in the spectrum of Al_{13}^-.

Our data support an electronic shell picture for the 3p band of Al_n^- with $n>13$. If these electronic shells can be explained by a modified jellium model [6] or if these shells correspond to the different symmetry dominating the cluster the structure cannot be decided based on the available experimental and theoretical data.

4. Conclusion

The development of the 3p valence band of small Al_n^- clusters with $n=2$–20 has been studied by means of photoelectron spectroscopy of cluster anions. We observed the mixing of the 3p band with a single particle orbital derived from the 3s band for Al_n^- with $n>8$. This partial s–p hybridization for these small clusters was not observed in earlier experiments [9,10]. It is observed simultaneously to the transition occuring between Al_5^- and Al_{11}^- from planar to 3D structure.

The spectra of clusters larger than Al_{13}^- indicate the development of electronic shells. For $n=14$–20 the spectra consist of two main features, the one at lower BE growing in intensity with increasing n. The increase of intensity corresponds to a gain of one valence electron per additional Al atom.

Acknowledgement

We thank R. Jones and Chia-Yen Cha for lively and encouraging discussions and H. Pfeifer and J. Lauer for their technical support.

References

[1] Proceedings of the Sixth International Meeting on Small Particles and Inorganic Clusters, Chicago, USA (16–22 September 1992) Z. Physik D 26 (1993).

[2] O. Echt, K. Sattler and E. Recknagel, Phys. Rev. Letters 47 (1981) 1121.

[3] W. de Heer, Rev. Mod. Phys. 65 (1993) 611.

[4] C.-Y. Cha, G. Ganteför and W. Eberhardt, J. Chem. Phys. 100 (1994), in press.

[5] R.O. Jones, Phys. Rev. Letters 67 (1991) 224; J. Chem. Phys. 99 (1993) 1194.

[6] T.H. Upton, Phys. Rev. Letters 56 (1986) 2168; J. Chem. Phys. 86 (1987) 7054.

[7] C.E. Moore, Atomic energy levels as derived from the analysis of optical spectra, NSRDS-NBS circular No. 35 (US GPO, Washington, 1971).

[8] W.A. Harrison, Electronic structure and the properties of solids (Freeman, New York, 1980).

[9] K.J. Taylor, C.L. Pettiette, M.J. Craycraft, O. Chesnovsky and R.E. Smalley, Chem. Phys. Letters 152 (1988) 347.

[10] W.A. de Heer, P. Milani and A. Chatelain, Phys. Rev. Letters 63 (1989) 2834.

[11] C.-Y. Cha, G. Ganteför and W. Eberhardt, Rev. Sci. Instrum. 63 (1992) 5661.

[12] P. Kruit and F.H. Read, J. Phys. E 16 (1983) 313.

[13] G. Ganteför, K.H. Meiwes-Broer and H.O. Lutz, Phys. Rev. A 37 (1988) 2716;
G. Ganteför, M. Gausa, K.H. Meiwes-Broer and H.O. Lutz, Z. Physik D 9 (1988) 253.

[14] U. Meier, S.D. Peyerimhoff and F. Grein, Z. Physik D 17 (1990) 209.

[15] H. Hotop and W.C. Lineberger, J. Phys. Chem. Ref. Data 14 (1985) 731.

[16] C.-Y. Cha, G. Ganteför and W. Eberhardt, Z. Physik D 26 (1993) 307; J. Chem. Phys. 99 (1993) 6308.